Ionospheric Variations in Response to Lightning Discharges and Their Parental Thunderstorms

Xuan-Min Shao[1*], Erin Lay[1], and Abram Jacobson[2]

1. Los Alamos National Laboratory, Los Alamos, NM 87545, USA
2. University of Washington, Seattle, WA 98195, USA

ABSTRACT: In this paper, we report our recent observations of the variations of ionospheric D-region electron density due to lightning discharges and due to electrically active parental storms. We will also report our recent observations of TEC (total electron content) fluctuations in the ionospheric F-layer related to mesoscale storms. For the D-region observations, we use VLF/LF time waveforms of lightning signals as probing sources and are able to detect the electron profile in a spatially and temporally-resolved manner. We found that electron density in the nighttime D-region was reduced significantly in response to lightning discharges atop a small storm, and the extent of the reduction is closely related in time and space to the rate of lightning discharges, supporting the EMP-enhanced electron attachment theories. On the other hand, an electrified storm as whole appears to steadily induce more electrons at the lower level in the nighttime D-region, apparently due to the static electrical field/current effect. Through these two competing processes the D-region electron density distribution could become highly inhomogeneous in space and time. The TEC variation near mesoscale storms were observed with an array of ground-based GPS (the Global Positioning System) receivers. We found that anomalous TEC variations are closely associated in time and space with mesoscale storms, apparently related to storm-produced acoustic-gravity waves. The largest variation is observed to be 1.4 TECU (10^{16} e/m^2) over a typical nighttime background value of several TECUs.

INTRODUCTION

Thunderstorms and their lightning discharges have been reported to disturb the lower ionosphere (D-layer) and possibly the upper ionosphere (F-region) by acoustic and atmospheric gravity waves, by electric field changes produced by lightning discharges, and by conduction current driven by thunderstorm's static electric field. However, many of the perturbative effects are not well understood due to the complexity of the coupling effects and the technical challenges of the relevant measurements.

Lightning-produced VLF radio signals had been previously used to probe the D-region electron density variations by examining the signals' waveguide mode propagation between the ground the D-region. This technique provides a lightning-to-receiver path-averaged observation of the D-region variations [Cummer et al., 1998; Han and Cummer, 2010a, b; Han et al., 2011]. Recently, Shao et al. [2013] and Lay et al., [2014] compare the observed VLF/LF time waveforms of lightning return strokes to the corresponding VLF/LF propagation simulations [Jacobson et al., 2009, 2012; Shao and Jacobson,

---

[1] Contact information: Xuan-Min Shao, Los Alamos National Laboratory, Los Alamos, NM 87544, USA, Email: xshao@lanl.gov

2009], and is able to derive the D-region electron density profiles in a spatially- and temporally-resolved manner. This time-domain technique that based on the features of the groundwave and the first-hop ionospheric reflection enables us to examine the D-region variations in a great detail, and some recent results are presented in this paper.

In addition to the D-region variations, correlated observations of thunderstorm activities and GPS TEC fluctuations show that thunderstorms could also introduce significant disturbances deeper into the ionosphere (F-region) where the bulk of electrons reside [Lay et al., 2013].

OBSERVATIONS

Using lightning VLF/LF signals to probe D-region electron density profile

Figure 1 illustrates the time-domain technique that uses the return stroke waveform to probe the ionospheric D-region. For a remote VLF/LF sensor (e.g., the Los Alamos Sferic Array, LASA, [Shao et al., 2006]), the groundwave signal arrives first, and the ionospheric signal arrives later after being "reflected" from the D-region at the midpoint between the lightning and the sensor. The relative time delay and amplitude ratio between the two signals depends on a number of VLF/LF propagation parameters from the source to the sensor, including the ground conductivity, the Earth's magnetic field at the reflection point, the collision frequency in the D-region, and the D-region electron density profile. All the parameters except the electron profile can be obtained independently and can be assumed constants in the time scale of the thunderstorm lifetime, and the variations in the received waveform is dependent on the variations of the D-region electron profile. Since only the first-hop reflection is concerned for the ionospheric signal, this technique only probes a small ionospheric area at the midpoint (Figure 1b), and therefore provides a localized measurement of the D-region.

To derive the electron profile, the measured return stroke waveform is compared to the modelled waveforms under assumptions of a range of different D-region electron profiles. In our analysis, the D-region profile is assumed to be the conventional exponential profile [Wait and Spies, 1964]
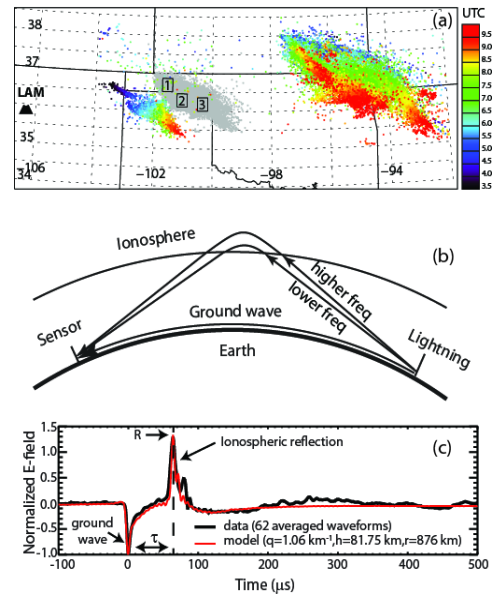

Figure 1. Use lightning VLF/LF signal to probe ionospheric D-region. (a) Probe gray area with lightning signals from mesoscale storm at the right and sensor (LAM) at left. (b) Illustration of ground and ionospheric waves from source to sensor. (c) Measured and modeled return stroke waveforms.
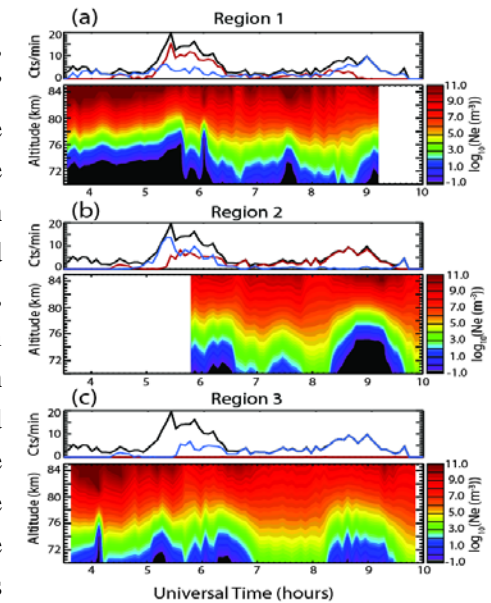

Figure 2. Variations of electron density atop of the small storm in Figure 1. (a) Top panel shows lightning rate of the small storm, and bottom electron density in log scale, for region 1 (Figure 1).   (b) and (c) same as (a) but for regions 2 and 3.

$$n_e(z) = n_0 e^{(-0.15h)} e^{(\beta-0.15)(z-h)} \qquad (1)$$

in which, $n_0 = 1.43 \times 10^{13}$ m^{-3}, h is the reference height in km, and β is the steepness of the profile in km^{-1}. Different pairs of (h,β) represent different profiles. The modelled waveform that best matches the observation indicates the most likely pair of (h,β) and therefore the most likely electron profile (equation 1). The red curve in Figure 1c shows the best matched modelled waveform for a specific measurement.

For the study presented in Shao et al. [2013], lightning return stokes from a mesoscale storm are used to probe the D-region atop a small storm that is situated approximately midway between the mesoscale storm and a LASA sensor (LAM). The gray dots next to the small storm are the midpoints and represent the probing area (Figure 1a). As discussed in detailed in Shao et al., [2013], the D-region electron density is observed to be reduced atop the small storm, and the extent of the reduction, in both space and time, is closely correlated with the lightning activity in the underlying storm (Figure 2).
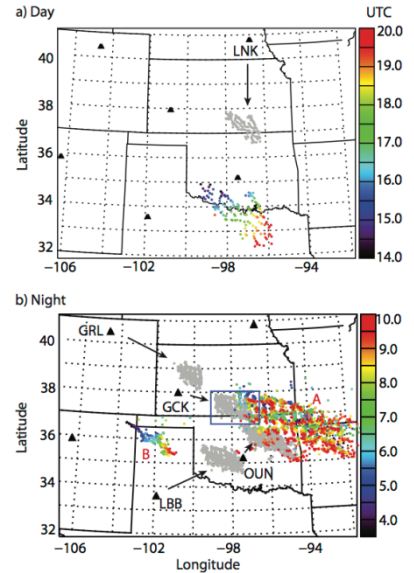

Figure 3. (a) Probe daytime D-region in the gray area. (b) Probe nighttime D-region around the storm from difference receivers, corresponding different gray areas.
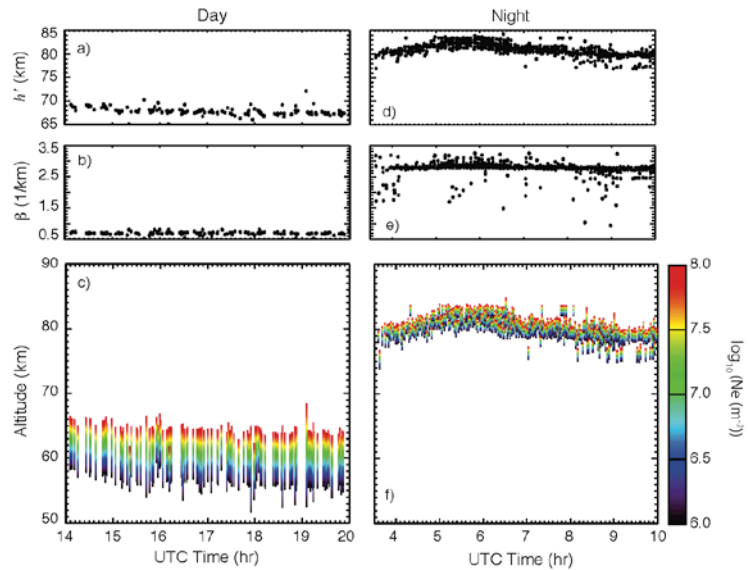
D-region electron profiles away from thunderstorm

Figure 3a depicts a probed area that is more than 200-km north of a mesoscale thunderstorm, and the probed area is not considered to be electrically affected by the storm. The observation is for a daytime D-region, between 14:00 and 20:00 UTC (9:00-15:00 local time). The derived electron profiles, h, β, and the exponential profile are shown in Figure 4a,b, and c respectively. No significant variation in the D-region is detected during the 6-hour period, except the slight and gradual descending of the region from the morning to the afternoon hours, as commonly observed for D-region.

Figures 4d, e, and f show an observation for a nighttime (3:30-10:00 UTC, or 22:30-5:00 LT) D-region that is more than 200-km away from the nearest thunderstorm. The gray area pointed from GRL in Figure 3b is the probed area for this observation. As commonly reported, the nighttime profiles are higher (h = 81km) and more steep ($\beta =$ 2.8 km^{-1}), and have more variations as compared to the daytime profiles.

Figure 4. D-region away from thunderstorms. Left, daytime ionosphere profiles, h, β, and the corresponding profiles. Colored lines represent density from 10^6 to 10^8 /m^3 in log scale. Right, same as left, but for a quiet nighttime D-region.

These profiles for the storm-"quiet" D-regions are in consistent with other *in situ* rocket observations, and can be considered to be background profiles for a "quiet" D-region.

D-region profiles disturbed by thunderstorms

In Figure 3b, the gray areas pointed from GCK, LBB, and OUN are above or nearer to the storms, and the corresponding D-region electron profiles are shown in Figures 5b, e, and f. Comparing these profiles with the "quiet" nighttime profiles of Figure 5a (the same as Figure 4f) it is immediately clear that they vary significantly and extensively. To compare the profile variations with thunderstorm activities, below each profile plot the lightning activities produced by the underlying storms are presented. As shown in Figures 5b and d for LBB, the profiles are very similar
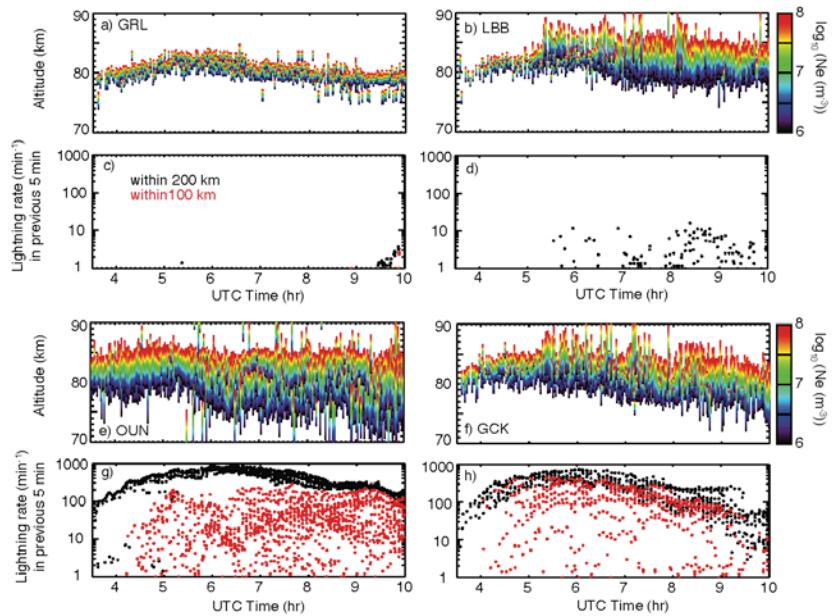

Figure 5. D-region atop or near thunderstorms. (a) Same as Figure 4f for quiet nighttime profiles. (c) Lightning events within 200 (black dots) 100-km (red) of probed area. (b) and (d) same as (a)and (c) but for probed area from LBB. Longer colored lines shows smaller steepness (β) for the profile. The other two groups are the same but for areas from OUN and GCK, as shown in Figure 3.

to the storm-quiet profiles (Figure 5a) up to 5:30 UTC when there is not lightning activity within 200-km of the probed area. When the storm moves within 200-km, the profile steepness (β) decreases (longer colour bars) and the electron density above 80-km is reduced, as compared to the "quiet" profiles. Figure 5e show the most significant variations with the increase of electron density at the lower region (<80 km) and decrease of electron density in the higher region (>80 km), and significant decrease of the steepness of the profiles, from $\beta = 2.8$ for "quiet" condition to 0.9 km^{-1}. The probed area for Figure 5e is indicated by the gray area pointed from OUN in Figure 3b, which is directly atop the southern partial of the storm. As also shown in Figure 5g a large number of lightning activities occur within 100-km (red dots) of the probed D-region during this time period.

F-region perturbations related to thunderstorms

In addition to the disturbances to the ionospheric D-region, thunderstorms have also been observed to be related to F-region (200-400 km altitude) perturbations [Lay et al., 2013]. To investigate this possible effect, ground-based GPS observations of total electron content (TEC) have been analysed. In Figure 6, the black curves are vertical TEC (VTEC) measurements from two different GPS stations. The general trend of the VTEC is determined by the solar angle, and the plots show the VTEC values decrease from high to low during the late afternoon hours. In order to investigate the possible perturbations related to the thunderstorms, the solar effect is detrended with a polynomial fit (the red curves in Figure 6), and the residual differences are examined.

Figure 7 shows the results for one of the cases presented in Lay et al. [2013]. Figure 7b shows the tracks of the pierce points viewed from ground GPS receivers to a GPS satellite, and the outline of a storm that occurred at the same time. Figure 7a shows the residual perturbations detected by the network of receivers. In this case, five stations (labelled red) detected clear TEC perturbations, and Figure 7b shows that the perturbations were detected northeast of the thunderstorm. The largest perturbation detected is on the order of ~1 TEC unit (10^{16} e/m^2) near 4:00 UTC, about 20% of the background TEC value.

CONCLUSIONS

Our recent observations show that thunderstorms in the troposphere can significantly disturb the ionosphere D-region and deeper into the F-region. The significant changes of D-region electron density profiles, especially those atop of mesoscale thunderstorms need to be considered in future sprites initiation simulations. In addition to the temporal variation illustrated in this paper, the disturbed D-region also shows highly inhomogeneous density distributions in space [Shao et al. 2013; Lay et al. 2014], which will enable the sprites to initiate below normal breakdown threshold.

F-region perturbations are likely related to thunderstorm-generated atmospheric gravity waves [Vadas and Crowley, 2010], but further correlated observational and model study is needed to better understand this phenomenon.

ACKNOWLEDGMENTS

REFERENCES

Cummer, S. A., U. S. Inan, and T. F. Bell, 1998: Ionospheric D region remote sensing using VLF radio atmospherics, *Radio Sci., 33*(6), 1781-1792, doi:10.1029/98RS02381.
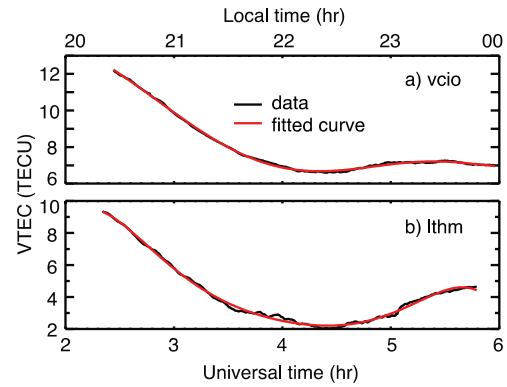

Figure 6. Black, VTEC from GPS measurement. Red, polynomial fit of black curves. The residual difference between black and red curves indicates perturbations.
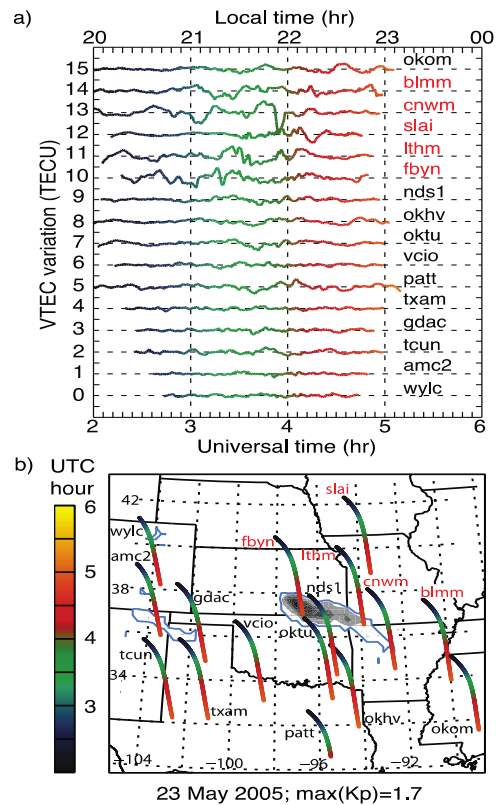

Figure 7. TEC perturbation observed over a thunderstorm. (a) Perturbations from individual GPS stations. (b) Tracks of measurements from a GPS network over the storm (outlined gray contours).

Han, F., and S. A. Cummer, 2010a: Midlatitude nighttime D region ionosphere variability on hourly to monthly time scales, *J. Geophys. Res., 115*, A09323, doi:10.1029/2010JA015437.

Han, F., and S. A. Cummer, 2010b: Midlatitude daytime D region ionosphere variations measured from radio atmospherics, *J. Geophys. Res., 115*, A10314, doi:10.1029/2010JA015715.

Han, F., S. A. Cummer, J. Li, and G. Lu, 2011: Daytime ionospheric D region sharpness derived from VLF radio atmospherics, *J. Geophys. Res., 116*, A05314, doi:10.1029/2010JA016299.

Jacobson, A. R., X.-M. Shao, and R. Holzworth, 2009: Full-wave reflection of lightning long-wave radio pulses from the ionospheric *D* region: Numerical model, *J. Geophys. Res., 114*, A03303, doi:10.1029/2008JA013642.

Jacobson, A. R., X. M. Shao, and E. Lay, 2012: Time domain waveform and azimuth variation of ionospherically reflected VLF/LF radio emissions from lightning, *Radio Sci., 47*, RS4001.

Lay, E. H., X.-M. Shao, and C. S. Carrano, 2013: Variation in total electron content above large thunderstorms, Geophys. Res. Lett., 40, 1945–1949, doi:10.1002/grl.50499.

Lay, E. H., X.-M. Shao, A. R. Jacobson, 2014: D-region electron profiles observed with substantial spatial and temporal change near thunderstorms, submitted to *J. Geophys. Res.*.

Shao, X.-M., and A. R. Jacobson, 2009: Model simulation of very low frequency and low frequency lightning signal propagation over intermediate ranges, *IEEE Trans. Electromagn. Compat., 51*, 519–525, doi:10.1109/TEMC.2009.2022171.

Shao, X.-M., M. Stanley, A. Regan, J. Harlin, M. Pongratz, and M. Stock, 2006: Total lightning observations with the new and improved Los Alamos Sferic Array (LASA), *J. Atmos. Oceanic Technol., 23*, 1273–1288, doi:10.1175/JTECH1908.1.

Shao, X.-M., E. H. Lay, and A. R., Jacobson, 2013: Reduction of electron density in the night-time lower ionosphere in response to a thunderstorm, *Nature Geoscience, 6*, 29–33.

Vadas, S. L., and G. Crowley, 2010: Sources of the traveling ionospheric disturbances observed by the ionospheric TIDDBIT sounder near Wallops Island on 30 October 2007, *J. Geophys. Res.*, **115**, A07324, doi:10.1029/2009JA015053.

Wait, J. R., and K. P. Spies, 1964: *Characteristics of Earth-Ionosphere Waveguide for VLF Radio Waves*, Natl. Bur. Stand., Boulder, Colo.